Lawrence Berkeley Laboratory
UNIVERSITY OF CALIFORNIA

Accelerator & Fusion Research Division

Presented at the Joint US–CERN School on Particle Accelerators, Isola di Capri, Italy, October 20–26, 1988

Electromagnetic Detectors

G.R. Lambertson

January 1989

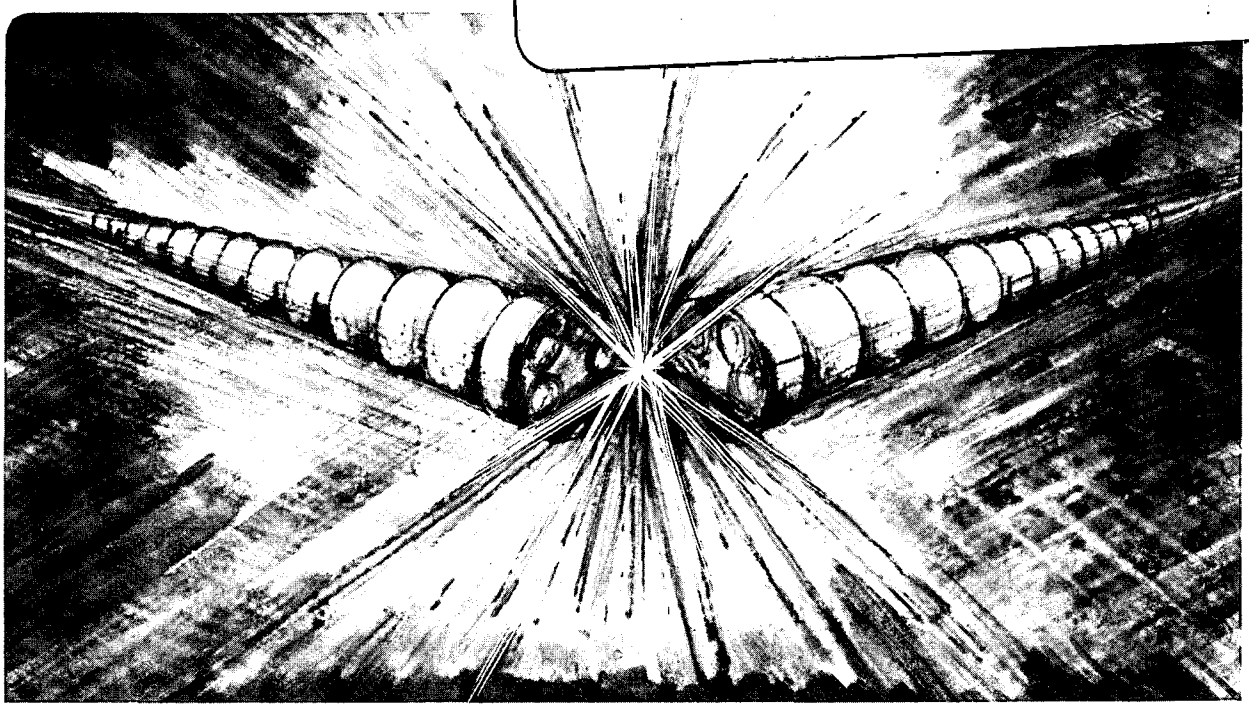

Prepared for the U.S. Department of Energy under Contract Number DE-AC03-76SF00098.

DISCLAIMER

ELECTROMAGNETIC DETECTORS*

GLEN R. LAMBERTSON
Accelerator and Fusion Research Division
Lawrence Berkeley Laboratory
1 Cyclotron Road
Berkeley, CA 94720 USA

1. INTRODUCTION

Monitors of the particle beams in accelerators are most commonly electromagnetic devices that extract a small amount of energy from the beam but are substantially non-interfering. Of course, one aspect of the design of such detectors is the avoidance of spurious strong interactions that are undesired. Before examining in some detail the principles of these devices some illustrative examples of detector types will be mentioned. A very common type is the "capacitance" pickup (Fig. 1) which consists of an antenna or surface that is exposed to the electric field of the beam and connected to a signal amplifier or monitor. Variations in the position or intensity of the beam change the induced charges in the exposed electrode and are monitored by the external circuit. A so-called "magnetic" pickup would be a loop of conductor exposed to the changing magnetic field of the beam. The loop may have a core of magnetic material for increased sensitivity. If the loop is made in the form of a two-conductor TEM transmission line as illustrated in Fig. 2, it becomes the stripline or directional coupler, as used in electronic circuitry. It has the property that if the beam particles and the wave in the line travel at the same velocity, for example, c, the induced signal appears only at the upstream end and the downstream termination of the line plays no part in its function. This directional behavior may be visualized as being a result of the combination of capacitive and magnetic effects, or alternatively as current waves induced into the ends of the line. Contrasting with this is the response of a disc-loaded waveguide or a helix in which an induced signal can build up as the beam moves along the structure if the guide phase velocity and the beam velocity are made alike. One should notice that in order to extract energy

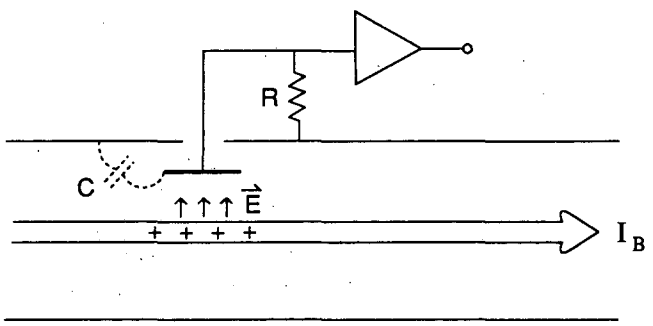

Fig. 1. Schematic capacitive pickup.

* This work was supported by the Director, Office of Energy Research, Office of High Energy and Nuclear Physics, High Energy Physics Division, U.S. Dept. of Energy, under Contract No. DE-AC03-76SF00098.

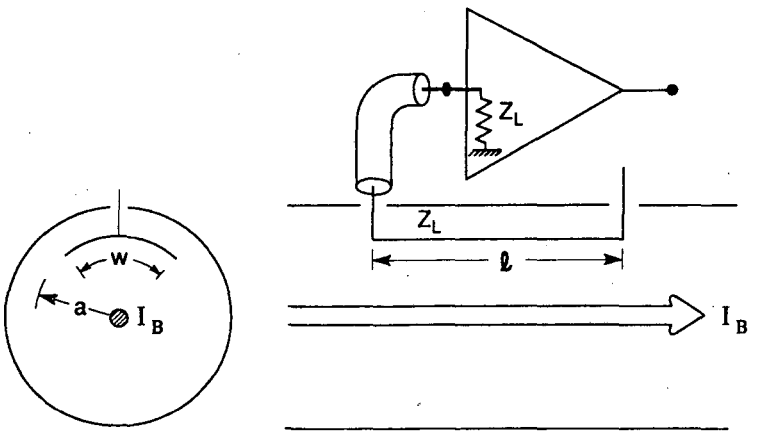

Fig. 2. Schematic stripline pickup.

from the fields of the beam, all these passive devices must in fact interact with the electric fields E, not the magnetic field, B. Also none has response down to zero frequency. To these rules there are a few exceptions, such as (1) the dc current transformer with a nonlinear magnetic material and active feedback, and (2) the deflection of a stream of electrons by the magnetic field of a beam. When excited by an external source, a pickup structure may be used as a kicker to produce a change in the longitudinal or transverse momentum of the particles in the beam.

2. RESPONSE FUNCTIONS

The electromagnetic detector is characterized primarily by the voltage, or power, available at its output terminal from a unit of beam current within some band of frequencies. A commonly used parameter is the transfer impedance, Z_P, which is the complex ratio of the voltage V_P produced to the current of the beam, I_B, at a given frequency.

$$Z_P(\omega, v) = \frac{V_P}{I_B}. \tag{2.1}$$

The wave of beam current in the longitudinal, s-direction is $I_B\, e^{j(\omega t - ks)}$, with velocity $v = \omega/k$. Because Z_P will be seen to depend upon the output impedance Z_C of the detector circuit, it is important to state if that value is different from the usual value $R_o = 50$ ohm. If the phase of the response is not needed, then a useful quantity that is independent of output impedance is the power, available at the output, which is

$$P_P = \frac{1}{2}\frac{|I_B Z_P|^2}{Z_C} = \frac{1}{2} I_B^2 \frac{R_\parallel T^2}{4}. \tag{2.2}$$

Here we have introduced $R_\parallel T^2$, the longitudinal shunt impedance times the square of the transit time factor for the electrode when used as a kicker. This quantity which is a convenient measure of efficiency will be discussed more later.

For a detector used to determine the transverse position x of a beam, the parameter of interest is the transverse impedance

$$Z'_P(\omega, v) = \frac{1}{I_B}\frac{dV_P}{dx} \tag{2.3}$$

usually written as

$$Z'_P = \frac{V_P}{I_B x} \tag{2.4}$$

for a beam displaced x away from a central position at which the detector output is zero. And, in analogy with the longitudinal case, we have the output power

$$P'_P = \frac{1}{2}\frac{|I_B x Z'_P|^2}{Z_C} = \frac{1}{2}(I_B x)^2 k^2 \frac{R_\perp T^2}{4} \tag{2.5}$$

in terms of a transverse shunt impedance $R_\perp T^2$.

3. CONCEPTS OF IMAGES AND INDUCTION, SOME EXAMPLES

In a straightforward approach to calculating the response of a pickup structure, one would assume that the motion of the beam particles is negligibly altered by their interaction with the pickup and then solve the electromagnetic boundary-value problem for the particular electrode geometry to obtain the voltages and currents in the electrodes. Except for very simple cases or for approximations, this can be an involved problem; for that reason, an alternative approach will be described later. However for pickup electrodes that are small compared to the wavelength of the signal, the concepts of image charges and currents and magnetic coupling are very useful; as intuitive solutions to boundary-value problems, these can guide one's understanding and inventiveness. For most accelerator applications, images in the conducting wall of the beam tube effectively duplicate in longitudinal distribution the currents in the beam. This correspondence between beam and image is in part a result of the relativistic foreshortening of the electromagnetic fields of high-velocity particles. Hence, if an electrode forms part of the beam tube surface we can estimate the charges and currents induced in it.

(a) Capacitive pickup. Apply this to the case of a small "button" electrode of area A on the surface of a beam tube of radius a. The linear charge density of the beam is $I_B/\beta c$; the button will then receive a charge

$$q = \frac{A}{2\pi a}\frac{I_B}{\beta c} \tag{3.1}$$

as a result of an induced current

$$\begin{aligned} i = j\omega q &= \frac{j\omega}{\beta c}\frac{A}{2\pi a} I_B \\ &= jklgI_B \end{aligned} \tag{3.2}$$

where we have introduced an effective length l and a coverage factor $g = A/2\pi al$ representing that fraction of the 2π angular space around the beam that is occupied by the electrode. This nomenclature will be useful later for larger electrodes. The response of the electrode of Fig. 1 is then the signal developed by this current in the RC circuit shown:

$$V_P = \frac{i}{\frac{1}{R} + j\omega C} = jk\frac{lg}{\frac{1}{R} + j\omega C} \tag{3.3}$$

and

$$Z_P = jk\frac{lg}{\frac{1}{R} + j\omega C}. \tag{3.4}$$

Above the frequency for which $\omega RC >> 1$ the capacitance effectively integrates the current to make the device a broadband monitor with response

$$Z_P \implies \frac{lg}{\beta cC}. \tag{3.5}$$

(b) Stripline. The image current is useful in explaining the basic features of the response of a stripline pickup (Fig. 2). In this geometry the stripline receives a fraction $g \sim \mathrm{w}/2\pi a$ of the image current. As a short pulse of the, assumed positive, beam current $i_B(t)$ reaches the upstream end, it repels positive charges into the output line and along the stripline. If the characteristic impedances of both these are Z_L, a prompt signal of $1/2\, Z_L g i_B(t)$ is seen at the output and an equal pulse propagates downstream with velocity c. At time l/c later the beam, assumed to have velocity c, and the pulse arrive at the downstream end where the departing beam releases into the stripline a negative pulse $-\,gi$. One half of this cancels the positive current traveling downstream and one half survives to propagate upstream. It enters the output line at time $2l/c$ and is seen as a negative pulse of voltage $-1/2\, Z_L g i$ (upper Fig. 3). It is now easy to see what signals are produced if the beam velocity βc were low. The output then will depend upon how the downstream end is terminated. In Fig. 3 are shown the signals for three cases of downstream termination. Lack of fidelity in the response results if reflections arise from imperfect impedance matching especially where the stripline joins the outgoing lines. The seemingly superfluous downstream matching resistor may be desired to absorb some of these reflections. If one Fourier analyzes the response for $\beta = 1$, the result is:

$$Z_P = Z_L g e^{j(\pi/2 - k_o l)} \sin k_o l \tag{3.6}$$

with $k_o = \omega/c$ and at output Z_L. This response is all real and a maximum at $k_o l = \pi/2$, i.e., at $l = \lambda/4$. For this reason the device is often called a "quarter-wave loop." Zeroes in the response occur when the line length is a multiple of one-half wavelength. (These zeroes may be removed if the signals from the downstream end can be suppressed; this has been done with ferrite absorbers

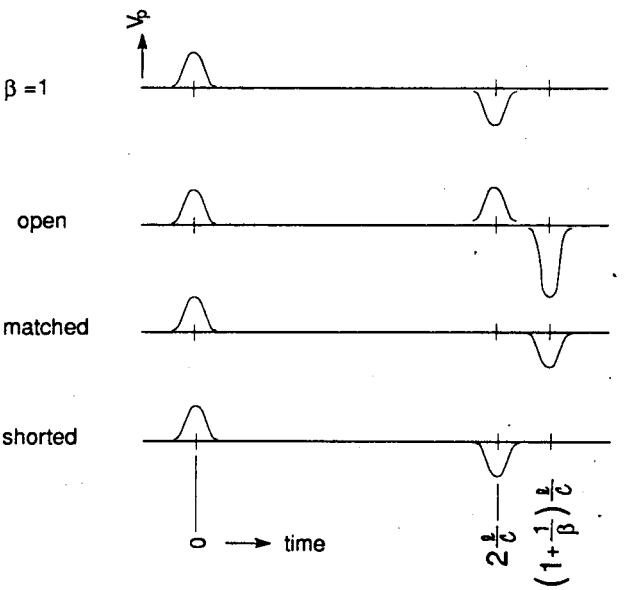

Fig. 3. Stripline signals for various back terminations.

and by exponentially tapering the cross section of the stripline.[1]) As sketched in Fig. 2 the output of the stripline would depend upon the position of the beam in the tube through variation of the geometric factor g. Hence the difference signal from two striplines located on opposing sides of the beam can be used to monitor transverse position. Conversely, the sum signal from such a pair is very weakly responsive to position, or if a single electrode is widened to completely encircle the beam so as to make $g = 1$ in Eq. 3.6, the signal is nearly independent of beam position up to frequencies for which the wavelength is comparable with the tube circumference.

(c) Magnetic loop. In the foregoing examination of the stripline loop, intuitively or by just knowing the answer we ignored effects of capacitive or magnetic induction in the central part of the electrode. It is true that these effects cancel or at least should not be added to the assumed image currents. But if the stripline were very short, it will be recognized as a magnetic pickup loop for which it would seem proper to consider the magnetic coupling to the beam current. To pursue that concept examine now the signal from a small loop made of a short stripline of conductor of width w enclosing area A. This loop at distance a from the beam will develop a voltage from dB/dt of

$$V_P = j\omega\mu_o \frac{A}{2\pi a} I_B = jk_o Z_o \frac{A}{2\pi a} I_B \,. \tag{3.7}$$

Here Z_o is the impedance $\mu_o c = 120\pi$ ohm. To compare this with Eq. 3.6 for the longer stripline, insert in that relation

$$Z_L \approx Z_o A/l\omega$$
$$g \approx \mathrm{w}/2\pi a$$
$$\sin k_o l \approx k_o l << 1$$

and we note that the result is identical to Eq. 3.7. Thus, magnetic loops are part of the stripline family. The magnetic coupling may be increased by forming the loop around a core of permeable material such as ferrite that partially or fully encircles the beam. This effectively increases the line impedance Z_L, lowers the line velocity, and shifts the first zero of the response to a lower frequency for a given line length. Nevertheless up to frequencies of about 400 MHz ferrite makes the stripline very compact. This feature has been applied in the pickups for stochastic cooling in the Antiproton Accumulator at CERN[2] for the frequency band 50-to-500 MHz.

(d) D.C. current transformer. The magnetic loop is, of course, a transformer and may be made with multiple turns around a core to provide a strong signal at high output impedance. The high impedance is not a problem for low signal frequencies and the beam current transformer has been developed for sensitive monitoring of the lower-frequency beam currents. The response of the current transformer can be extended down to zero frequency by detecting the nonlinear magnetization of a core of permalloy. One winding on the core is strongly excited with a modulator current at perhaps 250 Hz. This excitation of the core, sensed on a secondary winding, is analyzed for second harmonic content. Any net demagnetization by the beam current will magnetically bias the operating point on the $B - H$ curve of the core material and produce second harmonic. The second harmonic response is returned to zero by feedback to a third dc bias winding; the current required in that winding is then a measure of the dc beam current it is opposing. To avoid the 250 Hz modulation coupling to the beam, two oppositely-wound cores are used. This arrangement can measure dc and low frequency beam currents as small as a few μA. The frequency of the system may be extended by adding a third or more cores to sense the ac beam currents as shown in Fig. 4.[3] Rejecting contamination by the modulation frequency requires special circuits if the extended frequency response is desired.

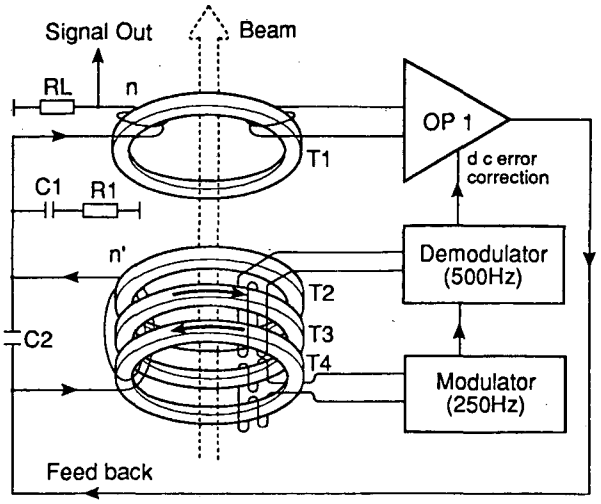

Fig. 4. DC current transformer circuit.

(e) Wall current monitor. If the conducting beam tube is interrupted by a gap, the ac image currents will develop a voltage across whatever external impedance bridges the gap. This external impedance may be an r.f. cavity for selected high frequencies or a band of resistors for a very broad frequency response. The resistively-loaded gap should be enclosed by an inductively-loaded cavity (Fig. 5) to avoid signals from sources external to the beam tube and to keep beam signals from radiating into the surrounding equipment. Typically the resistive band is an array of 50 or 100 resistors in parallel making a total resistance $R \approx 1$ ohm or less. The voltage developed across the gap is then RI_B and is sampled at two or four points around the circumference by 50-ohm cables. The low-frequency cutoff $\omega = R/L$ is limited by the inductance L of the ferrite-loaded cavity. The gap capacitance and parasitic inductances distort the high frequency response, typically limiting the usable frequency to about 1.5 GHz. Such a wall-current monitor will also show a difference in voltage across the diameter if a bunched beam passes in the tube off-center. At low frequencies this difference signal is reduced by azimuthal redistribution of the non-uniform wall currents flowing towards the gap. The gap can be viewed as an azimuthal slot line loaded by conductance per unit length of $G' = (2\pi aR)^{-1}$ and specific inductance L'.[4] Attenuation of currents flowing along this line will preserve the azimuthal distribution above a frequency for which

$$\omega L' 2\pi a > 8R. \tag{3.8}$$

(f) Resonant cavity. A detector with narrow band width would be formed by a gap loaded by a high-Q resonant cavity. The impedance offered to the wall current will be the shunt impedance of the cavity as loaded by the detector output load. One half of the power extracted from the beam is available as signal. But the analysis of a cavity is more adequately dealt with using the alternative method to which we now turn.

4. USEFUL THEOREMS

(a) Reciprocity. For obtaining the pickup impedance function, application of the Lorentz reciprocity theorem can transform the boundary-value problem containing the beam current into the usually easier calculation of the response of a beam when the structure is powered externally and used as an accelerating or deflecting electrode, commonly called a kicker. The calculation then

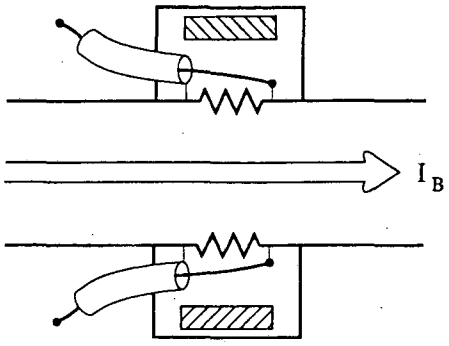

Fig. 5. Resistive wall-current monitor.

proceeds in three separable steps: first, the calculation or estimation of the longitudinal electric field along beam trajectory in the kicker, second, the evaluation of the integrated longitudinal electric field (kick) that would act upon a particle that travels upstream, and third, a simple multiplication of this kick by $Z_C/2$ to obtain the transfer impedance.

The reciprocity theorem relates the electromagnetic fields within a volume, which result independently from two different sources of excitation, in our case the kicker power supply and the beam current, designated by subscripts K and B. The volume is bounded by surface S. The basic form of the theorem, in which fields and currents are expressed as complex phasors or vectors with time dependence $e^{j\omega t}$, is[5]

$$\oint_S (\vec{E}_K \times \vec{H}_B - \vec{E}_B \times \vec{H}_K) \cdot d\vec{S} = \int_{vol} (\vec{E}_B \cdot \vec{J}_K - \vec{E}_K \cdot \vec{J}_B)\, d\, vol. \tag{4.1}$$

In the schematic diagram of a pickup in Fig. 6 the outgoing signal V_B generated by I_B is the pickup signal that earlier we have called V_P. The characteristic impedance of the signal port is Z_C; it may be a coaxial cable of this impedance. The inwardly traveling kicker driving voltage V_K is also at impedance Z_C. V_K produces the fields E_K and B_K and, only in resistive media in the structure, the currents J_K. This implies we ignore any perturbations of the beam current caused by the kicker fields. The volume integral vanishes in resistive media because $J = \sigma E$, leaving only the term in $E_K \cdot J_B$ containing free current. The portion of the surface integral covering the entrance and exit beam ports may be made zero if traveling waves are attenuated or the beam pipes are small enough to prevent propagation. At the signal port entering and exiting

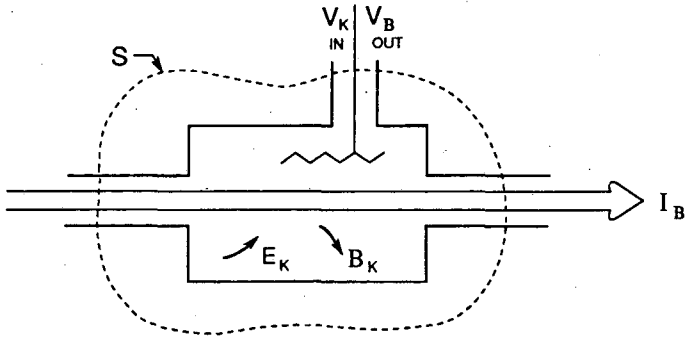

Fig. 6. Pickup diagram for application of reciprocity theorem.

TEM waves contribute to the surface integral two additive terms of $V_K V_B / Z_C$. If in an actual circuit V_B or V_K waves have reflections, we must exclude the reflected V_B signals because those arise outside the surface S. Reflections of the V_K waves are allowed but do not contribute to the surface integral. Therefore, Eq. 4.1 becomes

$$2\,\frac{V_K V_B}{Z_C} \;=\; -\int_{vol} \vec{E}_K \cdot \vec{J}_B \, d\,vol$$

or

$$V_B \;=\; -\frac{Z_C}{2V_K}\int_{vol} \vec{E}_K \cdot \vec{J}_B \, d\,vol\,. \tag{4.2}$$

In this equation, note that J_B is a sinusoidal wave of beam current and the integral is evaluated at one instant in time. It is clear that if we can calculate the s-directed fields in the pickup when it is excited by V_K from the outside, then Eq. 4.2 will give the pickup response.

The equation will be simplified if we assume that E_K does not vary greatly over the beam cross section and also insert the s-dependence e^{-jks} of J_B. Integrating over x and y gives

$$\int_{\perp} \vec{E}_K \cdot \vec{J}_B \, dx dy = \vec{E}_K \cdot \vec{I}_B \, e^{-jks} \tag{4.3}$$

and the pickup transfer impedance becomes

$$Z_P \;=\; -\frac{Z_C}{2V_K}\int_{s} e^{-jks}\,\vec{E}_K \cdot d\vec{s}. \tag{4.4}$$

This integral has a physical interpretation that we can recognize if we calculate the energy gain ΔU that a kicker imparts to a beam charge if the beam travels in the *negative* s sense.

$$\frac{\Delta U}{e} \;=\; \int_{s=b}^{a} e^{j\omega t}\,\vec{E}_K \cdot d\vec{s} \qquad \text{with} \quad s = -vt \tag{4.5}$$

$$\frac{\Delta U}{e} \;=\; \int_{b}^{a} e^{-jks}\,\vec{E}_K \cdot d\vec{s} \;=\; -\int_{a}^{b} e^{-jks}\,\vec{E}_K \cdot d\vec{s}\,. \tag{4.6}$$

But $\Delta U/e$ is just V_K times $K_\parallel$, the kicker constant; therefore comparing the above with Eq. 4.4, we see that

$$Z_P = \frac{Z_C \Delta U}{2eV_K} \;=\; \frac{1}{2}\,Z_C K_\parallel\,. \tag{4.7}$$

If we can evaluate the electrode's effectiveness as a kicker for particles moving upstream, then its response as a pickup for downstream current is also known.

(b) The voltage gain V. It will be convenient to give the voltage kick $\Delta U/e$ the symbol V and write the defining integral as applied to a particle moving in the positive sense of coordinate s.

$$V(x,y,k) \;=\; \int_{a}^{b} e^{jks}\,E_s ds \tag{4.8}$$

for the purpose of calculating electrode responses. The kicker constant K is then V/V_K and we simply remember that when used as a pickup the beam moves in the opposite sense. A position

detector will be designed to have a strong transverse variation of V, which produces the response through Eq. 2.3:

$$Z'_P = \frac{1}{2} Z_C \frac{dK_\parallel}{dx} = \frac{1}{2} \frac{Z_C}{V_K} \frac{dV}{dx} \tag{4.9}$$

The determination of the field E_s for use in calculating V is itself a boundary value problem but it does not involve the beam as a source. This is a considerable simplification especially if the beam velocity is less than c. Also, one can make use of all the techniques available for working with r.f. structures. It is for accelerating devices that the shunt impedance, noted in Eq. 2.2, is used in the equation for power dissipated:

$$P = \frac{V^2}{2R_\parallel T^2} = \frac{\omega W}{Q} \tag{4.10}$$

where W is the stored electromagnetic energy. The exponential factor in Eq. 4.8 brings in the transit-time factor.

In many cases the evaluation of V within the beam tube is made easier by knowledge of the field E_S at the wall of the beam tube. The electrode surfaces of a pickup often form part of the cylindrical beam tube surface and in that case, the potentials of those electrodes when excited as a kicker are calculable and therefore the longitudinal integrals of the electric fields are calculable at that surface. We examine next how to find $V(x, y, k)$ from its value on the cylindrical surface.

We wish to study the spatial variation of V within the beam tube. For this purpose and with greater generality let V now include the total time dependence of the field E_s rather than just one frequency component. The definition then becomes:

$$V(x, y, t) = \int_a^b E(x, y, s, t)\, ds \tag{4.11}$$

in which E is the s-directed field taken at the time $t = s/\beta c$ when the particle passes each value of s. This electric field must satisfy the wave equation

$$\nabla^2 E - \frac{1}{c^2} \frac{\partial^2 E}{\partial t^2} = 0. \tag{4.12}$$

Now we shall use this to find a two-dimensional differential equation involving the quantity

$$\nabla_\perp^2 V = \frac{\partial^2 V}{\partial x^2} + \frac{\partial^2 V}{\partial y^2}. \tag{4.13}$$

Differentiate Eq. 4.11 and insert Eq. 4.12:

$$\nabla_\perp^2 V = \int_a^b \nabla_\perp^2 E\, ds = \int_a^b \left(\frac{1}{c^2} \frac{\partial^2 E}{\partial t^2} - \frac{\partial^2 E}{\partial s^2} \right) ds \tag{4.14}$$

The variables s and t are related through $ds/dt = \beta c$, which we use in integrating Eq. 4.14 to obtain

$$\nabla_\perp^2 V = \left(-\frac{\partial E}{\partial s} = \frac{1}{\beta c}\frac{\partial E}{\partial t}\right)\Big]_a^b - \frac{1}{(\beta\gamma c)^2}\int_a^b \frac{\partial^2 E}{\partial t^2}\,ds\,. \tag{4.15}$$

The last term may be written in terms of V to give

$$\nabla_\perp^2 V + \frac{1}{(\beta\gamma c)^2}\frac{\partial^2 V}{\partial t^2} = \left(-\frac{\partial E}{\partial s} - \frac{1}{\beta c}\frac{\partial E}{\partial t}\right)\Big]_{a,t}^{t+(b-a)/\beta c}\,. \tag{4.16}$$

The spatial variation of V is determined by this Eq. 4.16. In many detectors or kickers, the limits a and b may be chosen to be where the fields are zero or alike, making the right-hand side zero. Equation 4.16 then simplifies to the modified wave equation

$$\nabla_\perp^2 V + \frac{1}{(\beta\gamma c)^2}\frac{\partial^2 V}{\partial t^2} = 0\,. \tag{4.17}$$

or if variation $e^{j\omega t}$ is assumed,

$$\nabla_\perp^2 V - \left(\frac{k}{\gamma}\right)^2 V = 0\,. \tag{4.18}$$

Note that while the velocity of the beam particles did not enter into determining the kicker fields in the peripheral cylinder surface, that velocity does enter into calculating V on that boundary and in the internal region through the factor γ in Eq. 4.18. If γ for the particle beam is large, Eq. 4.18 approaches Laplace's equation and then it is very convenient to use electrostatics to find the variation of V within the aperture.

(c) Panofsky-Wenzel. The effect of a kicker that deflects the beam is to produce a transverse momentum kick of $\Delta p_\perp$ per particle from an input kicker voltage V_K. Analogous to the integral defining V, we have for $\Delta p_\perp$

$$\frac{\Delta\vec{p}_\perp \beta c}{e} = \int_a^b (\vec{E}_\perp + \vec{v}\times\vec{B})e^{jks}\,ds\,. \tag{4.19}$$

A basic relation between V and Δp is provided by the Panofsky-Wenzel theorem[6]:

$$\frac{\partial V}{\partial x} = -j\omega\frac{\Delta p_x}{e}\,. \tag{4.20}$$

This theorem for any electromagnetic device in which the particle trajectory is essentially a straight line points out that for an interaction with the particle beam, there must be longitudinal electric fields or field gradients. A consequence of this is the fact that a structure with purely transverse electric fields, i.e., TE modes, cannot detect or kick a beam.

Further in analogy to the longitudinal kicker, we define $R_\perp T^2$ from the kicker power through the equations

$$P = \frac{1}{2}\frac{|V_K^2|}{Z_C} = \frac{1}{2}\frac{|\Delta P_\perp \beta c/e|^2}{R_\perp T^2} \tag{4.21}$$

Using Eqs. 4.9, 4.20, and 4.21 the real part of the pickup impedance is found in terms of the

transverse shunt impedance to be

$$Re\, Z'_P = \frac{k}{2}\sqrt{Z_C\, R_\perp\, T^2}\,. \tag{4.22}$$

5. RESONANT CAVITY

The cavity resonator, because of its high Q-value can be a very sensitive detector within its narrow frequency response band. For simple shapes the shunt impedance is readily calculated and, using the reciprocity relation, also gives the response as a detector. For example, a moderately-sized beam tube may be attached to the rectangular cavity as in Fig. 7 and it will retain the basic features of a closed-box cavity. The lowest cavity mode with maximum electric field along the centerline is mode TM_{110} for which the wavelength is $\sqrt{2}b$ and the electric field is

$$E \;=\; E_o \cos\frac{\pi x}{b}\;\cos\frac{\pi y}{b} \tag{5.1}$$

uniform in the s-direction.

To calculate $R_\parallel T^2$, we can use Eq. 4.10 for power absorbed by the cavity when driven at resonance. The quality factor Q applies to the unloaded cavity and W is the energy stored in the cavity given by

$$W \;=\; \frac{1}{2}\epsilon_o \int_{vol} E^2\, d\,vol\,. \tag{5.2}$$

Inserting E from Eq. 5.1, we find

$$W = \frac{1}{8}\epsilon_o\, E_o^2 b^2 l\,. \tag{5.3}$$

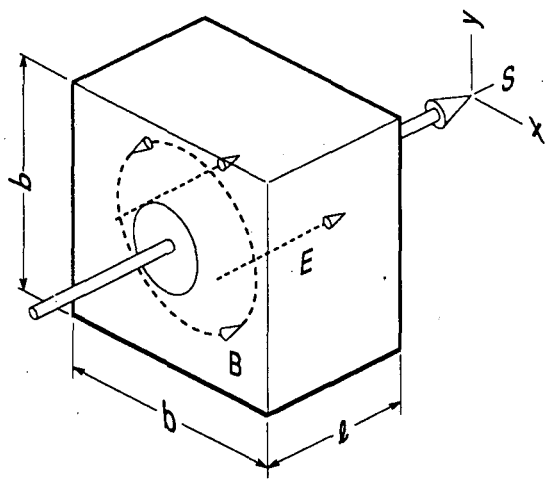

Fig. 7. Square cavity resonator.

For V we use Eq. 4.8 and the value of E at $x = y = 0$ to get

$$V = E_o l \frac{\sin\theta}{\theta} = E_o l T \tag{5.4}$$

with $\theta = \omega l/2v = k_o l/2\beta$ and $T = \sin\theta/\theta$. Insert W and V in Eq. 4.10 to find

$$R_\parallel T^2 = \frac{4}{\pi} Z_o \frac{l}{\lambda} Q T^2 = \frac{2}{\pi^2} Z_o \, k_o l \, Q T^2 \tag{5.5}$$

$$= 480 \frac{l}{\lambda} Q T^2 \,\text{ohm}. \tag{5.6}$$

As an example of another shape resonator, for a circular cavity (pillbox) with mode TM_{010}, for which the field is

$$E = E_o \, J_0 \, (kr), \tag{5.7}$$

one can find that

$$R_\parallel T^2 = \frac{2}{[\rho_{01} J_0(\rho_{01})]^2} Z_o \frac{l}{\lambda} Q T^2 \tag{5.8}$$

in which $\rho_{01} = 2.405$ giving

$$R_\parallel T^2 = 484 \frac{l}{\lambda} Q T^2 \text{ ohm}. \tag{5.9}$$

This result is nearly identical with that for the square cavity. For $\beta = 1$, a broad maximum in the quantity lQT^2/λ occurs at $\theta = 1.37$ radians for which $l/\lambda = 0.37$ and $T^2 = 0.51$. At that optimum length, the simple cavity then gives

$$R_\parallel T^2 = 108 \, Q \,\text{ohm}. \tag{5.10}$$

This can be increased about 25% by reducing the longitudinal gap in the region immediately surrounding the beam tube.

In these equations, the Q-factor for the unloaded cavity is used, which may be in the region of 30,000 at 1 GHz. For maximum efficiency, a matched coupling to an external load R_o typically 50 ohm, will reduce the Q of the circuit by a factor of 2. The peak response in terms of pickup impedance, using Fig. 2.2 is, still using the unloaded Q-value,

$$Z_P = \frac{1}{2}\sqrt{R_o R_\parallel T^2} \tag{5.11}$$

and using $R_o = 50$ ohm,

$$Z_P = 37\sqrt{Q}\,\text{ohm} \tag{5.12}$$

and $\Delta\omega/\omega = 2/Q$.

The peak response of a cavity used as a transverse detector is found from a calculation of $R_\perp T^2$. As for any resonator, the kicker power is $\omega W/Q$ and from Eqs. 4.20 and 4.21 we find

$$R_\perp T^2 = \left(\frac{1}{k}\frac{\partial V}{\partial x}\right)^2 \frac{Q}{2\omega W}. \tag{5.13}$$

The cavity of Fig. 7, if excited in the TM_{210} mode will have the longitudinal field

$$E = E_o \sin \frac{2\pi x}{b} \cos \frac{\pi y}{b} \tag{5.14}$$

and $\lambda = 2a/\sqrt{5}$. Use Eq. 4.8 to calculate $V(x)$. W and T are the same as in Eqs. 5.3 and 5.4 and we find using Eq. 5.13

$$R_\perp T^2 = \frac{32}{25\pi} Z_o \beta^2 \frac{l}{\lambda} Q T^2 \tag{5.15}$$

$$R_\perp T^2 = 153.6 \beta^2 \frac{l}{\lambda} Q T^2 \text{ ohm}. \tag{5.16}$$

At $\beta = 1$ the maximum value of lQT^2/λ occurs at $\theta = 1.41$ and gives

$$R_\perp T^2 = 33.7\ Q \text{ ohm}, \tag{5.17}$$

and from Eq. 4.22 into a 50-ohm load

$$Z'_P = 21\ k_o \sqrt{Q} \text{ ohm/m}. \tag{5.18}$$

In the foregoing, we assumed that the cavity fields were not altered by the beam tube apertures in the end walls. But there are small changes and, besides effects on the frequency and Q, the apertures affect the variation of sensitivity across the tube. To calculate this we can use Eq. 4.17 to find V within the aperture from values at the edge. As a well-known example, consider the circular cavity with attached circular tubes of radius a. With an azimuthally symmetric mode, the value of $V(r, \phi)$ at radius a will be the same for all values of ϕ. Call this value $V(a)$ and solve Eq. 4.17 with this boundary value. The result is

$$V(r) = V(a) \frac{I_o(k_o r/\beta\gamma)}{I_o(k_o a/\beta\gamma)}. \tag{5.19}$$

The modified Bessel function defines a reduced sensitivity at the tube center, unlike the function J_o that applies to the closed cavity, which is strongest at the center. The reduction is usually small; for fully relativistic particles it is zero and the sensitivity is perfectly uniform.

This approach can be applied to other cases if some estimate of the azimuthal variation of V at the tube radius is known. In that case, for each n^{th} azimuthal Fourier harmonic in $V(a, \phi)$, the radial dependence will be $I_n(k_o r/\beta\gamma)$.

To determine the pickup's response more exactly, one can calculate numerically reasonably simple cavities having nose cones and beam tubes. But to include the effects of the coupled external load and details of construction, measurements are needed. To measure this using a current-carrying wire to simulate the beam is complicated by the strong coupling if Q, and therefore RT^2, is large. But for the narrow-bandwidth structure, RT^2 and Z_P can be determined using the perturbing-bead method.

In the perturbation method, the cavity is excited at its resonant frequency ω. Then a small object of volume $\Delta\tau$ is introduced at a point on the beam trajectory and the change in resonant frequency $\Delta\omega$ is measured. If the scalar amplitudes of the field at the point where the object was placed were originally E and H, the perturbation is given by Slater[7,8] as

$$\frac{\Delta\omega}{\omega} = \frac{\Delta\tau}{4W}\left(\mu_o\alpha_h H^2 - \epsilon_o\alpha_e E^2\right) \tag{5.20}$$

The coefficients α_h and α_e are determined by the shape of the perturbing object. For small spheres (beads) of metal or of dielectric with $\epsilon = \epsilon_r\epsilon_o$, these are:

$$\text{metallic} \begin{cases} \alpha_h &= 3/2 \\ \alpha_{em} &= 3 \end{cases} \tag{5.21}$$

$$\text{dielectric } \alpha_{ed} = 3\,\frac{\epsilon_r - 1}{\epsilon_r + 2}\,.$$

In a longitudinal pickup with only s-directed field $E(s)$ on the beam trajectory, one can measure as a function of s the $\Delta\omega/\omega$ caused by a metallic bead and find from Eq. 5.20 for insertion in Eq. 4.8

$$\frac{E^2}{W} = -\frac{4Z_o c}{\alpha_{em}\Delta\tau}\,\frac{\Delta\omega}{\omega}\,.$$

Equation 4.10 then gives

$$R_\parallel T^2 = \frac{V^2}{2\omega W}\,Q = \frac{2Z_o Q}{k_o\alpha_{em}\Delta\tau}\left[\int\sqrt{-\frac{\Delta\omega}{\omega}}\,e^{jks}\,ds\right]^2 \tag{5.22}$$

which is numerically evaluated from measured data. The equation shows the unloaded Q factor, but the bandwidth when used would correspond to the loaded Q.

A transverse pickup cavity will not generally have a purely TM field; some transverse E appears in the neighborhood of the beam tube apertures. Then it is convenient if we can measure both $E_\perp$ and $H_\perp$ along a line where $E_\parallel$ is zero and evaluate the integral in Eq. 4.19. If we use a metal sphere and a dielectric sphere of the same size, we measure with the metal sphere $\frac{\Delta\omega}{\omega}\big|_m$ as in Eq. 5.20 using α_{em} and with the dielectric we measure

$$\frac{\Delta\omega}{\omega}\Big|_d = \frac{-\Delta\tau}{4W}\,\epsilon_o\alpha_{ed}\,E^2\,. \tag{5.23}$$

Solve these response equations for E and H and use Eqs. 4.19, 4.20, and 5.13 to calculate $R_\perp T^2$:

$$R_\perp T^2 = \frac{2Z_o Q}{k_o\alpha_h\Delta\tau}\left\{\int\left[\sqrt{-\frac{\alpha_h}{\alpha_{ed}}\,\frac{\Delta\omega}{\omega}\Big|_d} + \beta\sqrt{\frac{\Delta\omega}{\omega}\Big|_m - \frac{\alpha_{em}}{\alpha_{ed}}\,\frac{\Delta\omega}{\omega}\Big|_d}\right]e^{jks}\,ds\right\}^2 \tag{5.24}$$

A very sensitive detector for transverse motions or Schottky signals in the Tevatron has been made using a rectangular cavity,[9] 15 cm on each side machined from aluminum. Its characteristics as a Schottky detector are

$$f = 2.045 \text{ GHz}$$
$$Q = 9500$$
$$\frac{R_\perp T^2}{Q} = 29\ \Omega$$
$$Z'_P = 81 \times 10^3 \text{ ohm/m}$$
$$\text{Noise limit} = 4.2 \times 10^{-13} \text{ ampere meter}$$

6. CAPACITIVE PICKUPS

The various configurations of the capacitive electrode can be analyzed using reciprocity and the function V. An example is the long plate connected at its center to a resonant circuit as sketched in Fig. 8. Regard the plate as a center-driven open transmission line with characteristic impedance Z_L. The open line presents at its center the impedance $-1/2jZ_L\cot(k_o l/2)$ plus losses. Resonate this capacitive reactance with the external inductor and let R represent the total circuit losses without the matched output load resistor. In terms of the unloaded Q-value, then

$$R = \frac{1}{2} Q Z_L \cot(k_o l/2). \tag{6.1}$$

Let the excited circuit have voltage V_o at the center-tap. This will produce at the ends of the line $V_o\sec(k_o l/2)$ and the associated fields $E_s(s)$ at the beam will be concentrated at the ends of the TEM line at points separated by an effective length l. At each end the integral of $E_s\,ds$ is $\pm g\,V_o\sec(k_o l/2)$ in which g is a geometric factor determined by the transverse placements of beam and electrode. If the extent in the s-direction of each of these end fields is small relative to $\beta\lambda = 1/k$, then the value of V calculated from Eq. 4.8 is approximately

$$\begin{aligned} V &= \int e^{jks} E_s\, ds \\ V &= \frac{gV_o}{\cos(k_o l/2)} \left[-e^{-jkl/2} + e^{jkl/2}\right] \\ V &= j\, V_o 2g \frac{\sin(kl/2)}{\cos(k_o l/2)} \end{aligned} \tag{6.2}$$

We find $R_\parallel T^2$ from the power dissipated

$$P = \frac{V_o^2}{2R} = \frac{V^2}{2R_\parallel T^2} \tag{6.3}$$

giving

$$R_\parallel T^2 = 2\, Z_L\, g^2 Q \frac{\sin^2(kl/2)}{\cos(k_o l/2)\sin(k_o l/2)}. \tag{6.4}$$

As a pickup the available coupling impedance at resonance into R_o will be, using Eq. 5.11,

$$|Z_P| = g \sin(kl/2) \sqrt{\frac{R_o Z_L Q}{\sin k_o l}}. \tag{6.5}$$

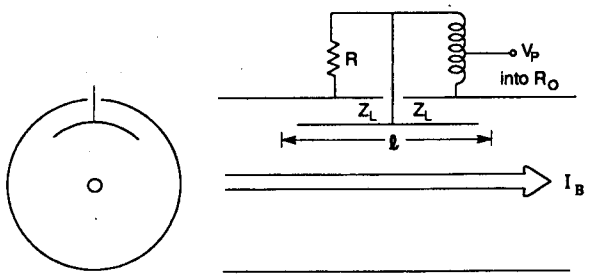

Fig. 8. Resonated capacitive plate.

For the short plate, it is sensible to write this in terms of the total capacitance C. Therefore insert $Z_L = l/cC$ to obtain

$$Z_P = \frac{gl}{2\beta c}\sqrt{\frac{\omega R_o Q}{C}}. \tag{6.6}$$

Comparing this resonated detector with the resistively-loaded and broader-bandwidth case given in Eq. 3.4 shows the reasonable result that the detector output power density has increased by at least a factor $Q/2$.

The factor g can be evaluated by solving, perhaps numerically, Eq. 4.18 for the distribution of V within the aperture cross section bounded by the beam tube and the electrode plate as in the axial view in Fig. 8. At the electrode plate, the value of V is Eq. 6.2 with $g = 1$. The solution for V depends upon the particle velocity βc. We see that strictly only if $\gamma = 1$ is that solution given by an electrostatic calculation.

The response of the detector to transverse beam position is found from $\nabla_\perp V$. A position detector will often have two or more plates. In this case, the interelectrode coupling (capacitances) must be included in calculating RT^2 and in the design of external circuits that select the difference signal.

A recent application of tuned-plate detectors for measuring the position of small extracted beam currents at Fermilab[10] has been able to resolve 0.1 mm with a beam current of 1.7×10^{-8} ampere with plates one meter long. The circuits operate at 53.1 MHz and have an unloaded Q of about 380.

A detector geometry used to obtain a linear response to transverse position, usually at low frequency, is that shown in Fig. 9. Two capacitive electrodes are formed by a diagonal cut through a section of beam tube. The arbitrary cross section sketched is intended to convey that the linear response is obtained with any shape cylindrical cross section. For electrodes small compared to $\beta\gamma\lambda$ this is true.

A proof of this may be demonstrated by applying Eq. 4.18 with the boundary values defined by the diagonal cut. For near linearity we must have $k_o l/\beta << 1$ and the excursion $x << \beta\gamma/k_o$.

The compact arrangement shown in Fig. 10 is used in the CERN PS to monitor horizontal and vertical positions and the total current.[11] The frequency range is 0.1 to > 200 MHz. The noise limit is ± 2 mm with 5×10^9 particles per bunch; at higher currents, the resolution limit is 0.1 mm.

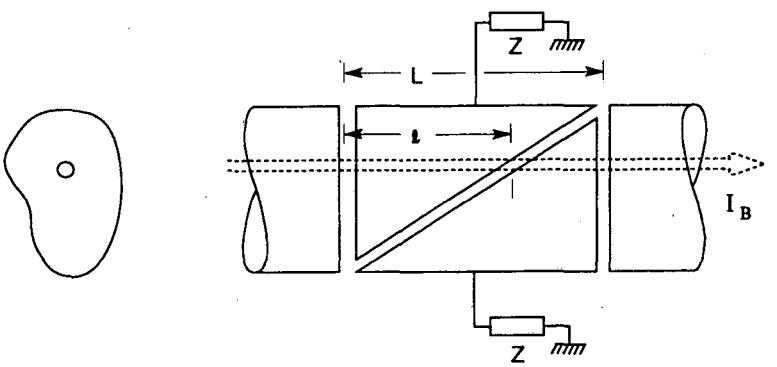

Fig. 9. Diagonally-cut cylinder pickup.

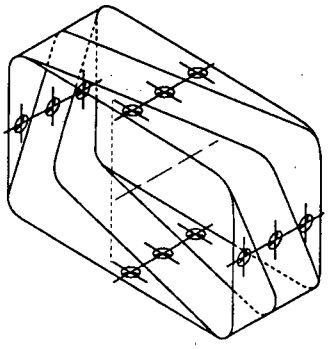

Fig. 10. Combined H and V electrodes.

7. THE STRIPLINE FAMILY

As we have seen, image-current concepts can give a good physical picture of the function of stripline detectors. But the stripline is so widely used as a broad-band detector that some supplementary analysis by the alternative method is worthwhile. Therefore, let us examine the pair of striplines sketched in Fig. 11 to be used as a sum current detector. Imagine the two lines, each of impedance Z_L and wave number $k_L = \omega/v_L$ driven in parallel from an $R_o = 50$ ohm source with voltage V_K. To provide the stripline voltages of V_L, a transformer is needed and the value of V_K required is $V_K = V_L\sqrt{2R_o/Z_L}$. For evaluating the function V, the voltage waves must travel in the negative s sense as noted in Section 4; thus the voltage at $s = -l$ is $V_L\, e^{-jk_L l}$ when it is V_L at $s = 0$. As with the capacitive plate, we visualize the E_s fields to be concentrated near $s = 0$ and $s = -l$ so that the integral for V is given approximately by

$$\begin{aligned} V &= g_{\|}\left[V(o)e^{o} \;-\; V(-s)e^{-jkl}\right] \\ V &= g_{\|}\left(1 \;-\; e^{-j(k+k_L)l}\right) \\ V &= 2\, g_{\|}\, V_L e^{j(\pi/2-\theta)}\, \sin\theta \end{aligned} \tag{7.1}$$

in which $\theta = (k + k_L)l/2$. The pickup impedance is now found using Eq. 4.7 to be

$$\begin{aligned} Z_P &= \frac{1}{2} R_o \frac{V}{V_K} \\ Z_P &= \sqrt{\frac{R_o Z_L}{2}}\, g_{\|} e^{j(\pi/2-\theta)}\, \sin\theta\,. \end{aligned} \tag{7.2}$$

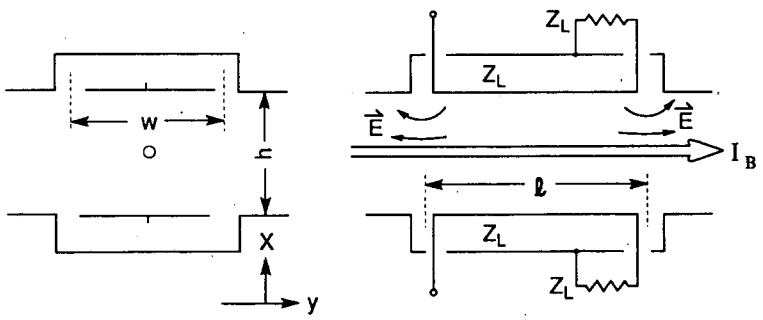

Fig. 11. Stripline pair.

This response is shown in Fig. 12. There are some differences between this result and Eq. 3.6 because here we have two lines driven from impedance R_o and the g-factor represents the coverage of the perimeter by the two lines combined; we also have separate values of k and k_L to allow for different velocities in the beam and the lines. The transformation to R_o does not appear in the response if it is given in terms of shunt impedance:

$$R_{\|}T^2 = 2\,Z_L\,(g_{\|}\sin\theta)^2\,. \tag{7.3}$$

The response of the pair of lines excited with opposite polarities when used as a position detector, obtained by differentiating Eq. 7.2, would contain $dg_{\|}/dx$, which we express as $g_{\perp}2/h$; this is written

$$Z'_P \;=\; \sqrt{\frac{R_o Z_L}{2}}\,g_{\perp}\,\frac{2}{h}\,e^{j(\pi/2-\theta)}\,\sin\theta \tag{7.4}$$

and

$$R_{\perp}T^2 \;=\; 2\,Z_L\left(\frac{2g_{\perp}}{kh}\,\sin\theta\right)^2\,. \tag{7.5}$$

But we must note that when used with a difference signal, the coupling between lines is smaller and the impedance Z_L must be reduced accordingly.

Long arrays of many stripline pickups have been used in beam cooling rings at CERN and at Fermilab. In this case it was necessary to design the gain-vs.-position to fit a particular function, using the spatial variation of g for the recessed plates shown in Fig. 10. In this case $V(x,y)$ is an electrostatics problem with a rather simple analytic solution. At the center point $x = y = 0$ between plates the g-factors are:

$$g_{\|} \;=\; \frac{2}{\pi}\,\tan^{-1}\left(\sinh\frac{\pi \mathrm{w}}{2h}\right) \tag{7.6}$$

$$g_{\perp} \;=\; \tanh\frac{\pi \mathrm{w}}{2h}\,. \tag{7.7}$$

The electrodes used in the Fermilab antiproton accumulator[12] are in arrays of 128 loop pairs with signals delayed and combined in phase. The striplines have $Z_L \approx 100$ ohm, $Z_P = 40$ ohm per pair, and are used in the band 1-to-2 GHz. For most applications, it is convenient to use

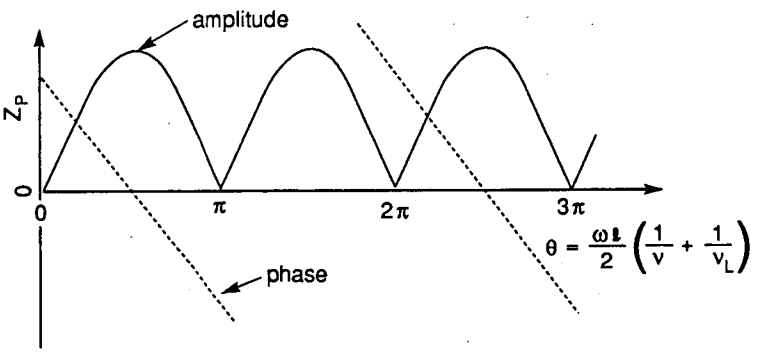

Fig. 12. Response of stripline pickup.

lower line impedance. Typical stripline electrode pairs have

$$\begin{aligned} Z_L &\approx 25 - 100\ \Omega \\ g &\geq \frac{1}{2} \\ Z_P &\approx 18 - 35\ \Omega \\ R_\parallel T^2 &\approx 25 - 100\ \Omega\,. \end{aligned}$$

Because stripline electrodes are directional couplers and have terminals at both ends, their signals may be added by simple series connection. Such an array is shown in Fig. 13. The sinusoidal signals, progressing upstream add in phase if the closely-spaced loops are $\lambda/4$ long at mid-band and the connecting transmission lines, all of impedance Z_L, are $\lambda/2$ long. Assume $v_B = v_L = c$, then the response of two strings each with n loops is just n times Eq. 7.2 but with a transit-time factor that defines a more narrow bandwidth:

$$Z_P = \sqrt{\frac{R_o Z_L}{2}}\, n\, g_\parallel\, T \tag{7.8}$$

in which

$$T = \frac{\sin 2n\phi}{2n\cos\phi}\, e^{j(\pi/2-(2n-1)\phi)} \tag{7.9}$$

with $\phi = k_o l_o = k_o l/n$. The bandwidth $\Delta\omega$ within half-power frequencies is, for $n \geq 2$ approximately $0.9\ \omega/n$.

This series array provides flexibility to exchange bandwidth for gain, much as we have by resonating the capacitive pickup. This has been applied in the CERN antiproton accumulator[13] where the reduced bandwidth arrays were desired to match power amplifier bandwidths. The electrode unit consists of two loops in series.

We can examine the series-connected loops here to illustrate the general rule that the product of peak power gain and bandwidth is proportional to the pickup length. For series loops of total length l, one can show that, with $T = 1$,

$$R_\parallel T^2 \Delta\omega \approx \frac{3.6}{\pi} Z_L c (k_o g_\parallel)^2\, l\,. \tag{7.10}$$

Some other examples of this product are:

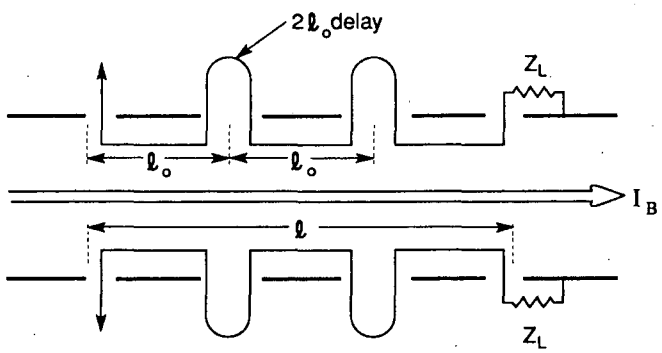

Fig. 13. Series loops.

Resonated capacitive strip pair (for $\beta = 1$):

$$Z_L c(k_o g_\parallel)^2 \frac{\tan(k_o l/2)}{k_o/2} \tag{7.11}$$

Square cavity:

$$\frac{4}{\pi^2} Z_o c \left(\frac{\beta \sin(kl/2a)}{l/2}\right)^2 l. \tag{7.12}$$

8. TRAVELING-WAVE DEVICES

A linear array of pickups with signals properly phased and combined creates a traveling wave of impedance to extract energy from the moving particle. But in this case, the signals are added in external combiners that add powers, not voltages. In a true traveling-wave structure such as a waveguide or a helical line there is the possibility of building up signal voltage proportional to length and hence power proportional to the square of length. This can be realized but with some loss in bandwidth caused by dispersion in the phase velocity. An additional attraction of traveling-wave structures is their lesser complexity as rf structures, particularly at frequencies in the multi-gigahertz range.

On the axis of a helical line Fig. 14, there is a longitudinal electric field with reduced velocity $\beta_L c$.[14,15] The shunt impedance of this electrode treated as a sheath helix is given by

$$R_\parallel T^2 = \frac{Z_o}{2\pi\beta_L} \left(\frac{h}{\gamma_L}\right)^2 \left[\frac{K_o(ha)}{I_o(ha)} - \frac{K_o(hb)}{J_o(hb)}\right] \left(\frac{\sin\theta}{\theta}\right)^2 \tag{8.1}$$

in which $\gamma_L^2 = \frac{1}{1-\beta_L^2}$, $h = \frac{k_L}{\gamma_L} = \frac{k_o}{\beta_L \gamma_L}$, and $\theta = (k - k_L)\,\frac{l}{2}$. The modified Bessel functions I_o and K_o for small arguments, that is, for $\beta_L \gamma_L \lambda > b$ reduce to the form

$$R_\parallel T^2 = \frac{Z_o}{2\pi\beta_L} \ln\frac{b}{a} \left(\frac{k_L l}{\gamma_L^2} \frac{\sin\theta}{\theta}\right)^2. \tag{8.2}$$

In this we recognize $(Z_o/2\pi)\ln(b/a)$ as the impedance of a coaxial line of radii a and b. Also, we see $\sin\theta/\theta$ as the transit-time factor in which t is a measure of the phase slip between beam and traveling wave. To avoid large dispersion in the wave velocity in this periodic structure, $\beta_L \lambda$ must be greater than twice the pitch of the helix. In an example use,[16] the helix was effective at $f = 200$ MHz and $\beta = 0.5$. However, the factor γ_L^{-4} makes the device ineffective for very relativistic particles.

The slotted-coax coupler shown in Fig. 15 communicates with the beam tube through a row of holes or slots in the outer wall of a coaxial line parallel to the beam. There is a net energy transfer from a beam particle to the coaxial line until either an equilibrium is reached or a sufficient phase

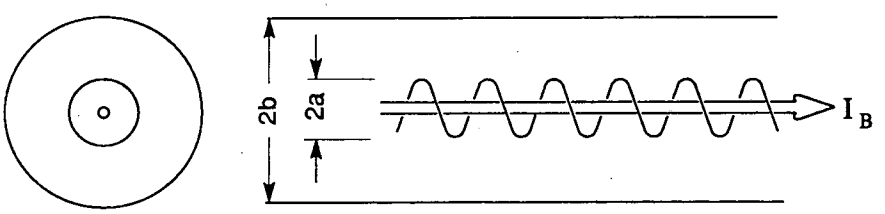

Fig. 14. Beam on axis of helical line.

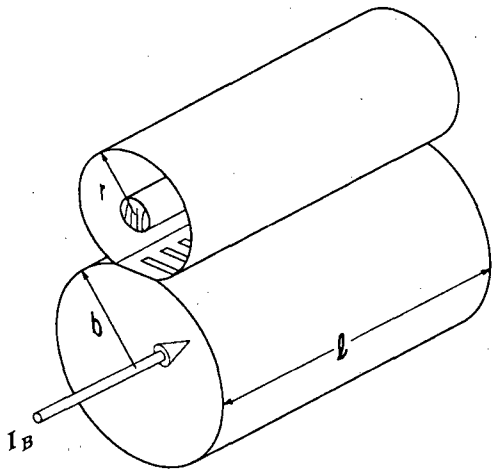

Fig. 15. Slotted coax on beam tube.

difference develops between beam and coax signal. The slots that provide the coupling also reduce the phase velocity in the coax and cause dispersion in that velocity. Perturbation calculations[17] for the geometry of Fig. 15 show that the coupling and the velocity are so related that the pickup impedance becomes simply

$$Z_P \;=\; -j\sqrt{R_o Z_L}\,\frac{k_o l r}{2\gamma_L^2 b}\,e^{-j\theta}\,\frac{\sin\theta}{\theta} \tag{8.3}$$

where Z_L is the impedance of the coax and γ_L and θ are as in Eq. 8.1. The shunt impedance is then

$$R_\parallel T^2 \;=\; Z_L\Big(\frac{k_o l r}{\gamma_L^2 b}\,\frac{\sin\theta}{\theta}\Big)^2 . \tag{8.4}$$

This is very similar to the result for the helix, but here a very small velocity reduction introduces dispersion that limits the use of the slotted coupler as a broad-band device to $\beta_L >\sim 0.95$. Although it is a weak coupler, it is a good high-frequency structure and is useful where strong coupling is not demanded. In this role it has been used in cooling the antiproton stack in the CERN AA ring.[18]

The phase velocity of a TM waveguide may be reduced to correspond to beam velocity by loading its walls with dielectric or corrugations. Linacs employ such structures. A corrugated guide has been developed[19] for experiments on stochastic cooling in the CERN SPS. This difference pickup is sketched in Fig. 16. It has a bandwidth of about 1 GHz at an operating frequency of 11 GHz. It has transverse shunt impedance of

$$R_\perp T^2 \;=\; 1.76\times 10^4 \text{ ohm}$$

and

$$Z'_P \;=\; 108 \text{ ohm/mm}.$$

This performance is exceptionally strong compared with the other types of pickup. The aperture is 16×22.9 mm and the length of the guide is 0.3 meter. The loaded guide is rather straightforward but the transition from guide to coax has required some development.

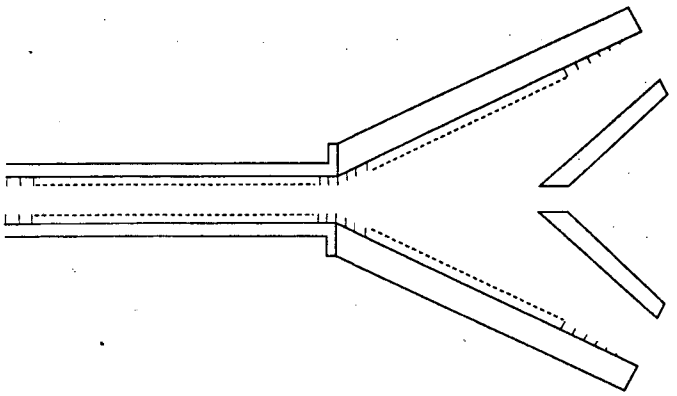

Fig. 16. Downstream end of corrugated-guide pickup.

We can inquire if the TW structure also has a gain-bandwidth product proportional to length. But for reference, first consider the standing-wave device with bandwidth $\Delta\omega = 2\omega/Q$ in terms of the unloaded quality factor. Its kicker power is given by Eq. 4.10

$$P = \frac{V^2}{2RT^2} = \frac{\omega W}{Q}.$$

From these relations, we find

$$RT^2\Delta\omega = \frac{V^2}{W} \tag{8.6}$$

which is proportional to length as we have seen for some particular cases. The equivalent starting point for the TW structure is

$$P = \frac{Wv_g}{l} \tag{8.7}$$

where v_g is the group velocity in the structure. The shunt impedance is then

$$R_\parallel T^2 = \frac{V^2 l}{2v_g W}. \tag{8.8}$$

To find the band width, we shall equate the transit time factor to $1/\sqrt{2}$ at $\pm\Delta\omega/2$. T is given by

$$T = \frac{1}{l}\int_{-l/2}^{l/2} e^{jks}\, e^{-jk_L s}\, ds = \frac{\sin\theta}{\theta} \tag{8.9}$$

where $\theta = (k_L - k)l/2$. At $\pm\Delta\omega/2$, θ has the value $\theta = \theta_1 = \pm 1.39$ radian. To first order we have

$$\theta_1 \approx \frac{\Delta\omega}{2}\frac{d\theta}{d\omega} = \frac{\Delta\omega l}{4}\left(\frac{dk_L}{d\omega} - \frac{dk}{d\omega}\right). \tag{8.10}$$

Using $k = \omega/v_B$ and $dk_L/d\omega = 1/v_g$, we find

$$\Delta\omega \approx \frac{4\theta_1}{l}\left(\frac{1}{v_g} - \frac{1}{v_B}\right)^{-1} \tag{8.11}$$

Combining this with Eq. 8.8 and the value of θ_1, we get

$$RT^2\Delta\omega \approx \frac{V^2}{W}\frac{2.8}{1-\frac{v_g}{v_B}}. \tag{8.12}$$

Here we see again a factor proportional to length; furthermore comparison with Eq. 8.6 also shows that indeed the TW structure could reasonably be a much stronger pickup than the standing-wave types. This last relation stands as a guide for the further development of TW devices as beam detectors.

REFERENCES

1. T. Linnecar, "The High Frequency Longitudinal and Transverse Pickups Used in the SPS," CERN-SPS/ARF/78-71 (August 1978).
2. S. van der Meer, "Stochastic Cooling in the CERN Antiproton Accumulator," IEEE Trans. Nucl. Sci. **NS-28**, 1994 (June 1981).
3. K. Unser, "A Toroidal DC Beam Current Transformer with High Resolution," IEEE Trans. Nucl. Sci. **NS-28**, 2344 (June 1981).
4. G.C. Schneider, "A 1.5 GHz Wide-Band Beam-Positron and Intensity Monitor for the Electron-Positron Accumulator (EPA)," Proc. of the 1987 IEEE Particle Accelerator Conference, Vol. 1, 664 (March 1987).
5. R.E. Colin, *Foundations for Microwave Engineering*, pp. 56–59, (McGraw Hill, 1966).
6. W.K.H. Panofsky and W.A. Wenzel, Rev. Sci. Instr. **27**, 967 (November 1956). G.R. Lambertson, "Dynamic Devices–Pickups and Kickers," *Physics of Particle Accelerators*, Eds. M. Month and M. Dienes, AIP 153, Vol. 1, p. 1413 (1987).
7. J.C. Slater, *Microwave Electronics*, Van Nostrand, Princeton, NJ, (1950).
8. E.L. Ginzton, *Microwave Measurements*, McGraw Hill, New York, NY (1957), pp. 445–449.
9. D.A. Goldberg and G.R. Lambertson, "A High-Frequency Schottky Detector for Use in the Tevatron," Proc. of the 1987 IEEE Particle Accelerator Conference, **1**, 547 (March 1987), Lawrence Berkeley Laboratory Report LBL-22273.
10. Q. Kerns et al, "Tuned Beam Position Detector for the Fermilab Switchgard," Proc. of the 1987 IEEE Particle Accelerator Conference, **1**, 661 (March 1987).
11. J. Durand et al., "New Electrostatic Pickups for the PS," presented at European Particle Accelerator Conf., Rome, (June 1988), CERN/PS 88-42 (PA) (June 1988).
12. D. Goldberg, G. Lambertson, F. Voelker, and L. Shalz, "Measurement of Frequency Response of LBL Stochastic Cooling Arrays for TEV-I Storage Rings," IEEE Trans. Nucl. Sci. **NS-32**, 2168 (October 1985), Lawrence Berkely Laboratory Report LBL-19564.
13. B. Autin et al., "Applications of Microwaves to Antiproton Control," Alta Frequenza, Vol. 56, **N10**, 381 (December 1987).
14. G. Lambertson, "The Helix as a Beam Electrode," Lawrence Berkeley Laboratory, Internal Report BECON-60 (August 1985).
15. H. Yonehara, et al., INS-NUMA-49 (1983).
16. G. Lambertson, et al., "Experiments on Stochastic Cooling of 200 MeV Protons," IEEE Trans. Nucl. Sci. **NS-28**, 2471 (June 1981), Lawrence Berkeley Laboratory Report LBL-11753.
17. G. Lambertson, K.J. Kim, and F. Voelker, "The Slotted Coax as a Beam Electrode," IEEE Trans. Nucl. Sci. **NS-30**, 2158 (August 1983), Lawrence Berkeley Laboratory Report LBL-15136.
18. J. Bosser, et al., "Design and Performance of the AAC Stack Core Cooling System," Presented at European Particle Accelerator Conference, Rome (June 1988), CERN/PS/88-25 (AR).
19. D. Boussard and G. DiMassa, "High Frequency Slow Wave Pickups," CERN-SPS/86-4(ARF), (February 1986).

LAWRENCE BERKELEY LABORATORY
TECHNICAL INFORMATION DEPARTMENT
1 CYCLOTRON ROAD
BERKELEY, CALIFORNIA 94720